



Spectrophotometric Investigations of Charge Transfer Complexes formed between imidazoles and DMAD

Pratibha Mittal*, Manisha Patni*, Raakhi Gupta*

Abstract

novel charge transfer (CT) complexes synthesized between imidazole-based donors and dimethyl acetylenedicarboxylate (DMAD) as the electron acceptor at room temperature in dichloromethane and acetone. CT complex formation was confirmed by characteristic $n \to \pi^*$ and $\pi \to \pi^*$ electronic transitions in UV-Vis spectra. Stoichiometric analysis using Job's method revealed 1:1 and 2:1 donor-acceptor ratios for imidazole and N-methylimidazole, respectively. Among the synthesized complexes, those containing N-methylimidazole displayed higher stability constants, negative Gibbs free energy changes (ΔG^0), and molar extinction coefficients (ϵ), reflecting spontaneous as well as stable complexation. Additionally, the lowest CT transition energies (E_{CT}) in dichloromethane confirmed stronger donor-acceptor interactions in the less polar solvent. DFT calculations at the B3LYP/6-31+G(d) level were carried out to further validate donor strength. N-methylimidazole exhibited the greater HOMO energy, low HOMO-LUMO energy gap (ΔE) and the most favourable global reactivity descriptors - chemical softness and chemical potential-affirming its better electrondonating ability compared to imidazole.

Keywords: Imidazole, DMAD, UV studies, DFT studies, Global reactivity descriptors, FMO analysis

1. Introduction

Organic charge transfer (CT) complexes are interesting materials and found broad range of applications in organic electronics [1, 2, 3, 4, 5] conductive materials [6] nonlinear optical (NLO) materials [7, 8] and in optoelectronic devices such as photodetectors and photoconductors [9, 10]. CT complexes are also reported to be used as biosensors for the non-destructive analysis

^{*} Department of Chemistry, IIS (Deemed to be University), Jaipur, 302020, Rajasthan, India; mittalpratibha073@gmail.com, <a href="mailto:mailt

of biological molecules, due to their high sensitivity and selectivity [11, 12]. Furthermore, they have demonstrated catalytic activity [13] in various chemical processes, including photochemical [14] and electrochemical reactions [15]. More recently, their potential in molecular memory devices has attracted interest, given their ability to switch between distinct electronic states [16].

Five-membered nitrogen-containing heterocycles are frequently employed as electron donors in CT complexes due to their aromatic character, delocalized π-electrons, and the presence of available lone pairs, all of which facilitate efficient charge transfer interactions [17]. Among these, imidazole has emerged as a particularly effective donor, outperforming other heterocycles such as pyrrole, pyrazole, and triazole. This enhanced donor ability is attributed to the presence of a pyridine-like nitrogen atom bearing a free lone pair, that participates in electron donation. In addition to its electronic properties, imidazole plays key roles in acid-base chemistry [18, 19], catalysis [20, 21], hydrogen bonding [22, 23], and metal ion coordination [24, 25, 26]. In biological systems, the imidazole moiety of histidine has been identified to bind metal ions including Cu(II) in metalloproteins [27]. Imidazole derivatives also show a wide range of biological activity, including antiviral, antitumor, antimicrobial, and antihistaminic effects, and are industrially used as corrosion inhibitors [28, 29, [30].

Despite containing two strong electron-withdrawing ester groups conjugated with a triple bond, dimethyl acetylenedicarboxylate (DMAD) is considered a moderate electron acceptor due to the $-\text{CO}_2\text{Me}$ substituents, which not only exhibit an electron-withdrawing nature but also exert resonance stabilization and partly delocalization of electron density away from the alkyne bond. Moreover, the linear carbon-carbon triple bond (alkyne bond) in DMAD offers less effective π^* overlap compared to the extended conjugated systems of classical acceptors like DDQ, TCNE, or TCNQ, which can be observed by the lower values of reduction potential and electron affinity. This electronic structure also lowers its LUMO energy, enabling efficient interaction with HOMOs of electron-rich donors to yield partial charge-transfer associations [31].

DMAD-based CT complexes are less prevalent in literature, making them an attractive subject for novel investigations to uncover subtle donor-acceptor behavior. In this view, we propose to use a clear, sensitive, and easy spectrophotometric method to create imidazole-DMAD CT complexes in the current study and investigate their stoichiometry, formation constants and transition energy spectrophotometrically.

Although several CT complexes of imidazole with organic acceptors such as chloranil, iodine, 3,5-dinitrobenzoic acid, 7,7,8,8-tetracyano quinodimethane (TCNQ), tetrathiafulvalene (TTF), oxalic acid, 2,4-dinitro-

1-naphthol, 2,3-dichloro-5,6-dicyano-1,4-benzoquinone (DDQ), and tetracyanoethylene (TCNE) [32, 33, 34, 35, 36, 37, 38, 39, 40] have been documented, no studies involving dimethyl acetylenedicarboxylate (DMAD) as an acceptor have been reported to date. Literature reports have, however, confirmed the use of imidazole-based charge transfer complexes in diverse applications, including spectroscopy, sensing, molecular electronics, and bioinorganic modeling, which underscores the significance of exploring DMAD as a novel π-acceptor in this context [41].

2. Methodology

2.1. Experimental Study

2.1.1. Materials and Instrumentation

All solvents and chemicals used in this study were of analytical and spectroscopic grade. Imidazoles (donor), dimethyl acetylenedicarboxylate (acceptor), and solvents (dichloromethane, acetone) were acquired from **Sigma-Aldrich (USA)** and further processed without purification. Absorption spectra of the UV-vis were obtained on a Shimadzu UV-1800 spectrophotometer with quartz cuvettes and a wavelength range of 200–800 nm

2.1.2. Preparation of stock solutions

Standard solutions (1×10⁻² M) of donors (imidazole and N-methylimidazole) and the acceptor (DMAD) were prepared in 50 mL volumetric flasks using dichloromethane and acetone as solvents. To determine their absorption maxima, equal volumes of donors (imidazole and N-methyl imidazole) and acceptor (DMAD) were scanned separately and then mixed in a 1:1 ratio to synthesize four CT complexes (1a-b, 2a-b) in both solvents (dichloromethane and acetone). The synthesized complexes were spectrophotometrically characterized to determine their have values.

2.1.3. Analysis of stoichiometric ratio

Spectrophotometric analysis based on Job's continuous variation method was used to evaluate the stoichiometry of the CT complexes. Master solutions were prepared and analyzed by mixing donors and acceptor in equal concentrations in both dichloromethane and acetone. 0.2-0.8 mL aliquots of solutions of donor and acceptor were used to make the total volume 1 mL, which was further diluted with the respective solvent [42].

2.1.4. Analysis of formation constant and molar extinction coefficient

Mole-ratio technique was employed in the determination of the formation constants and molar extinction coefficients of the synthesized charge transfer complexes. In this method, the concentrations of acceptor were varied and kept greater than the donor while keeping concentration of donor constant.

Benesi Hildebrand equation (as shown equation 1) was used facilitated the calculation of formation constant (K_{CI}) and molar extinction coefficient (\mathcal{E}) of the synthesized charge transfer complexes.

$$\frac{[D]_0}{A} = \frac{1}{K_{CT}\varepsilon} \cdot \frac{1}{[A]_0} + \frac{1}{\varepsilon} \quad \text{Or} \quad \frac{[A]_0^2[D]_0 \ l}{A} = \frac{1}{K_{CT}\varepsilon} + \frac{([A]_0 + 4[D]_0)}{\varepsilon}$$

$$\tag{1}$$

In this equation, A = absorbance

l = path length (1 cm).

[D]₀ and [A]₀ = baseline concentrations of donors and acceptor

By plotting the graph between $[D]_0$ /A v/s $1/[A]_0$ or $[A]_0^2[D]_0 1$ /A v/s $([A]_0 + 4[D]_0)$, a straight line was obtained, the slope and intercept of the graph depicted the formation constant and molar extinction coefficient respectively [43].

2.1.5. Determination of standard free energy (ΔG^0) and transition energy (E_{CT})

The ΔG^0 values (free energy change) [44] of all investigated complexes were calculated from the equation (2):

$$\Delta G^0 = -RT \ln K_{CT} \tag{2}$$

R = gas constant

T = temperature in Kelvin degrees

The charge transfer energy (E_{CT}) [45] of the formed CT complexes was calculated using the following equation (3):

$$E_{CT} = 1243.667/\lambda_{CT} \text{ nm}$$
 (3)

 λ_{CT} = absorption maxima of synthesized complexes.

2.2. Theoretical Study

Gaussian 16 software package was used to validate the results obtained from the experimental studies. These computational investigations were carried out at Density Functional Theory (DFT) at the B3LYP/6-31G(d) level. Geometry optimizations of donors and acceptors in gas phase and solvent was done using PCM model. The frontier molecular orbital (FMO) analysis was used to investigate the energy gap of HOMO (Donor) and LUMO

(acceptor), through which global reactivity descriptors were also determined by the following relations [46, 47, 48].

HOMO-LUMO energy gap (
$$\Delta E = E_{LUMO} - E_{HOMO}$$
) (4)

Hardness (
$$\eta$$
) = $\frac{E_{LUMO} - E_{HOMO}}{2}$ (5)

Softness (S) =
$$\frac{1}{\eta}$$
 (6)

Chemical potential (
$$\mu$$
) =
$$\frac{E_{HOMO} + E_{LUMO}}{2}$$
 (7)

Electronegativity
$$(\chi) = -\mu$$
 (8)

Electrophilicity index (
$$\omega$$
) = $\frac{\mu^2}{2\eta}$ (9)

Maximum electron transfer(
$$\Delta N max$$
) = $-\frac{\mu}{\eta}$ (10)

3. Results and Discussion

3.1. Experimental results

Table 1 summarizes the absorption maxima of the donor and acceptor; each recorded individually in dichloromethane and acetone using a UV–Vis spectrophotometer. Upon mixing equal volumes (2 mL each) of donor and acceptor, a yellow to bright red-colored charge transfer (CT) complexes were formed. The resulting solutions were scanned in the 200–800 nm region after 30 minutes. As shown in Table 1, new absorption bands appeared in regions where donor and acceptor did not exhibit absorption, indicating CT complex formation. These bands are attributed to $\pi \to \pi^*$ transitions (330–402 nm) and $n \to \pi^*$ transitions (454–508 nm), requiring different energy levels.

The higher-energy absorption bands (330–402 nm) involve electronic excitations from bonding π orbitals to antibonding π^* orbitals, which are allowed transitions with high molar absorptivity and occur at shorter wavelengths. In contrast, the lower-energy bands (454–508 nm) correspond to $n \to \pi^*$ transitions, where nonbonding lone pair electrons (usually from nitrogen or oxygen) are excited to π^* orbitals; are partially forbidden,

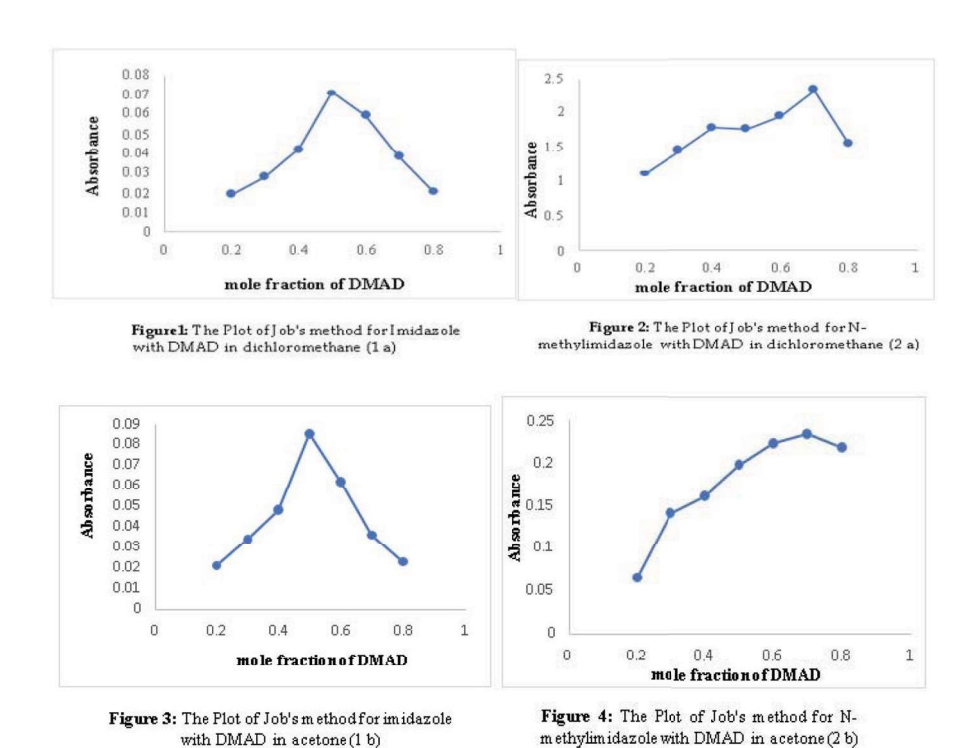
resulting in weaker absorption and longer wavelength bands.

Stoichiometric composition of the CT complexes was assessed through Job's method of continuous variation. The corresponding plots for the interactions of imidazoles with DMAD in dichloromethane and acetone are shown in Figures (1–4). The results indicated donor–acceptor ratios of 1:1 for imidazole and 2:1 for N-methylimidazole CT complexes in both solvents.

The difference in stoichiometry between imidazole–DMAD (1:1) and N-methylimidazole–DMAD (2:1) arises from the stronger electron-donating ability of N-methylimidazole. The N-methyl group increases ring electron density and HOMO energy, enabling DMAD to accommodate two donor molecules through sequential donor–acceptor interactions. Additional stabilization may also result from weak non-covalent contacts (π – π or C–H $\cdot\cdot$ O interactions).

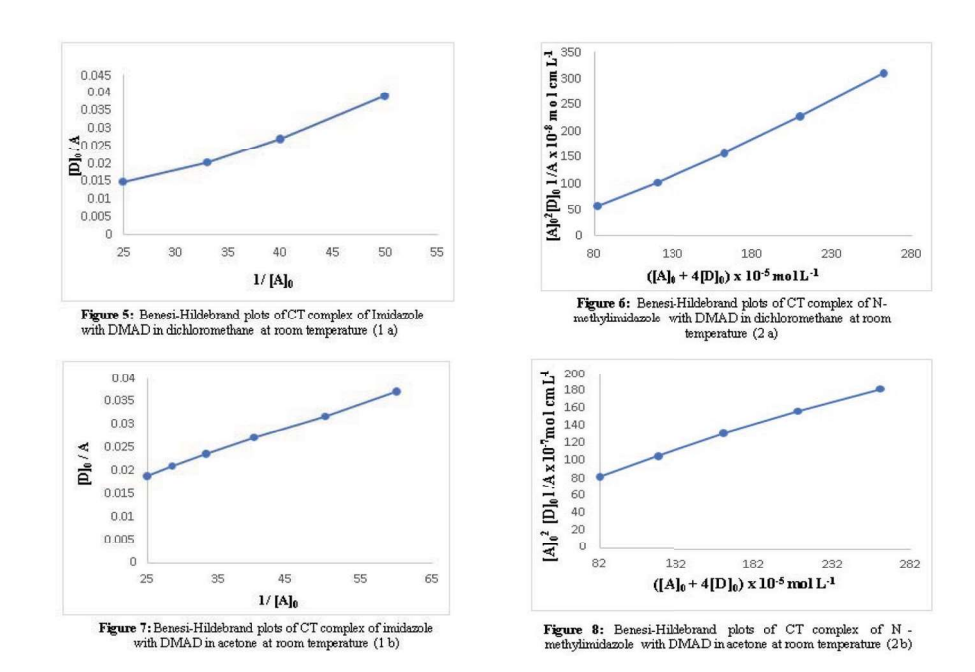
Table 1: Spectrophotometric data for the charge transfer complexes in dichloromethane and acetone

CT Complex	Imidazole (D): DMAD (A) (1a)	dazole (D): DMAD (A) (2a)	Imidazole (D): DMAD (A) (1b)	N-methylimi- dazole (D): DMAD (A) (2b)		
	In dichlo	romethane	In Acetone			
λ _{max} (nm) (donor)	273	234	275	234		
λ _{max} (nm) (Acceptor)	234	238	238	236		
λ _{CT} (nm)	330 454	354 506	336 459	402 508		
K _{CT} (mol ⁻¹)	12.0×10^2	22.0×10^2	4.14×10^2	6.98×10^2		
ε (cm ⁻¹ mol ⁻¹)	0.689×10^2	8.003×10^2	0.526×10^2	1.75×10^2		
E _{CT} (eV)	2.709	2.448	2.739	2.457		
ΔG ⁰ (KJ mol ⁻¹)	-6.154	-19.052	-3.518	-16.223		



It is evident from the Table 1 that CT complexes of N-methylimidazole exhibited the higher K_{CT} and ϵ values, confirming its superior donor strength to imidazole in both solvents. The solvent-dependent variation in the formation constants can be attributed to differences in polarity, dielectric constant, and solvation effects of dichloromethane (DCM) and acetone. Dichloromethane, being less polar ($\epsilon\approx 8.9$) and having a lower dielectric constant, favors stronger donor–acceptor interactions between imidazole derivatives and DMAD, thereby enhancing complex stability and resulting in higher K_{CT} values. In contrast, acetone is more polar ($\epsilon\approx 20.7$) and can solvate both donor and acceptor molecules effectively, which weakens the donor–acceptor charge-transfer interaction, leading to lower formation constants. These results underline the crucial role of solvent polarity and solvation in modulating CT complex stability [49].

The linear plots further supported these observations and found to be consistent with the spectral data presented in Figures (5–8).



The high negative Gibbs free energy (ΔG^0) confirmed the spontaneous generation of imidazole-based charge-transfer systems, whereas the greatest decrease in ΔG^0 is accompanied by the minimum transition energy (E_{CT}) reflected robust interaction between N-methylimidazole and DMAD.

3.2. Theoretical Results

The global reactivity descriptors of donor calculated with the help of equation 4-10, given in section 2.2, are presented in Table 2

Table 2: Global reactivity descriptors for optimized geometries of imidazoles at DFT level using B3LYP/6-31+G(d) basis set in gas phase and solvent

Molecule	Imidazole			N-methyl imidazole			
	Gas phase	DCM	Acetone	Gas phase	DCM	Acetone	
E _{HOMO (au)}	-0.238	-0.241	-0.242	-0.233	-0.238	-0.239	
E _{LUMO (au)}	-0.007	0.008	0.009	-0.004	0.004	0.004	
ΔE_{au}	0.231	0.249	0.251	0.229	0.242	0.243	
$\Delta \mathrm{E_{eV}}$	6.299	6.781	6.820	6.233	6.584	6.600	
η_{eV}	3.149	3.390	3.410	3.116	3.292	3.300	
S _{eV} ⁻¹	0.318	0.295	0.293	0.321	0.304	0.303	
μ_{eV}	-3.338	-3.171	-3.164	-3.235	-3.187	-3.198	

$\chi_{ m eV}$	3.338	3.171	3.164	3.235	3.187	3.198
$\omega_{ m eV}$	1.769	1.483	1.468	1.679	1.543	1.549
ΔNmax	1.060	0.935	0.928	1.038	0.968	0.969

The optimised geometries of imidazoles and their energy gap is also presented in the Figure 9 and 10 respectively.

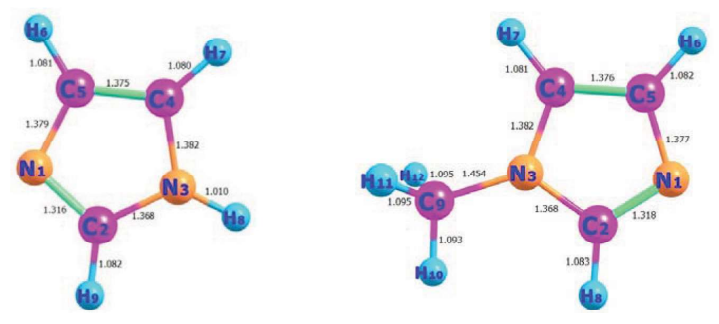


Figure 9: Optimized geometries of imidazole and N-methyl imidazole

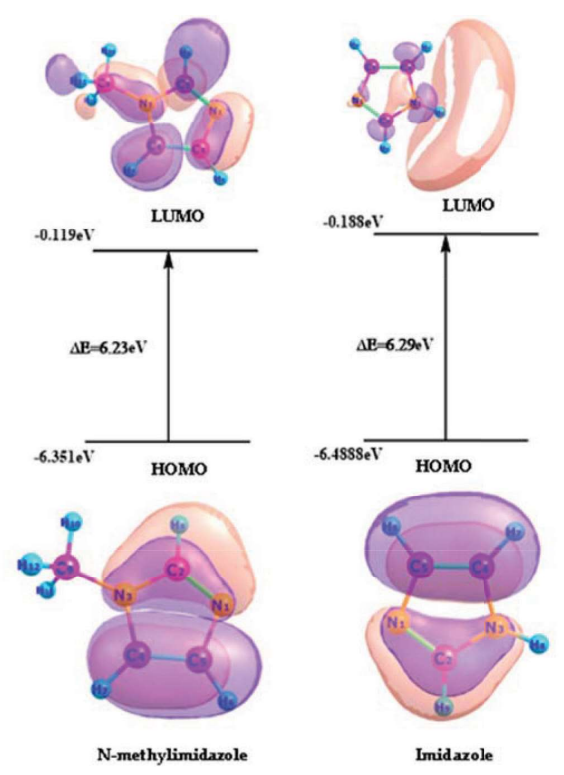


Figure 10: The HOMO-LUMO energy diagrams of imidazoles at B3LYP/6-3l+G(d) level in gas phase.

It is observed from the Table 2, that the ΔN max values (maximum electron transfer) confirmed both molecules are capable donors, but the high HOMO energy and low HOMO–LUMO gap (ΔE), indicated the better electron-donating ability of N-methylimidazole. Methyl substitution enhances electron density on the nitrogen atom, promoting stronger charge transfer interactions with DMAD. DFT-derived descriptors, including higher softness (S), less negative chemical potential (μ), and increased electrophilicity (ω), further supported its enhanced reactivity. In contrast, imidazole showed lower HOMO energy and less favorable reactivity indices, consistent with its lower K_{CT} and ϵ values. Overall, the results demonstrated that presence of electron releasing group improve donor strength and CT complex formation ability.

To know the strength of charge transfer complexes of imidazole-DMAD, FMO analysis has also been carried out theoretically at the same level in gas phase and in both solvents i.e. DCM and acetone. The energy difference between HOMO of donor and LUMO of acceptor was calculated in all four complexes. The findings are compiled in Table 3.

Table 3: HOMO (donor)-LUMO (acceptor) energy difference of synthesised CT complexes

Com- pound	HOMO (eV)			LUMO (eV)			HOMO (donor) - LUMO (acceptor) energy gap (eV)		
	Gas phase	Acetone	DCM	Gas phase	Acetone	DCM	Gas phase	Acetone	DCM
Imidazole	-6.488	-6.574	-6.561	-0.189	0.246	0.219	4.315	4.417	4.414
N-methyl imidazole	-6.351	-6.498	-6.479	-0.119	0.102	0.105	4.178	4.341	4.332
DMAD	-8.254	-8.435	-8.417	-2.173	-2.157	-2.147	-	-	-

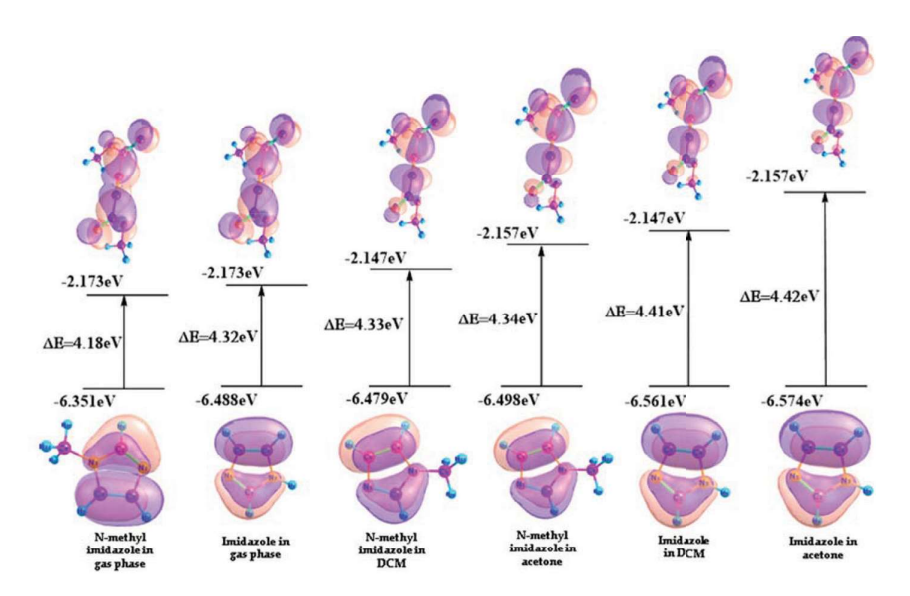


Figure 11: The HOMO-LUMO energy diagrams of imidazoles- DMAD CT complexes

It is evident from Table 3, that imidazole and N-methylimidazole act as strong electron donors with high-lying HOMOs, whereas DMAD serves as a π -acceptor with a low-lying LUMO. FMO calculations revealed that upon complexation, the HOMO-LUMO energy gap (ΔE) decreases in both solvents compared to the gas phase, confirming stabilization of the CT complexes. Orbital plots showed, the HOMO is localized on the donor and the LUMO on DMAD, validating the HOMO (donor) \rightarrow LUMO (acceptor) electron transfer pathway. Among the studied systems, the N-methylimidazole-DMAD complex in DCM exhibited the lower ΔE (4.33eV), consistent with its strongest donor ability. Figures 11 and 12 depict the optimized geometries and frontier molecular orbital (FMO) distributions of the imidazole-DMAD and N-methylimidazole-DMAD complexes, illustrating the electron density transfer and donor-acceptor interaction behavior discussed above.

Considering both experimental findings and theoretical calculations, the probable mechanism and structures of the synthesized CT complexes are outlined below:

$$H_3CO$$
 CH_3
 CH_3

Figure 12: (a)1:1 CT complex of imidazole with DMAD (b) 2:1 CT complex of N-methylimidazole with DMAD

4. Conclusions

The present study successfully demonstrated the formation and charge transfer complexes characterization of (CT) imidazole derivatives and dimethyl acetylenedicarboxylate (DMAD). Spectrophotometric and DFT analyses consistently revealed that N-methylimidazole is the most efficient electron donor, as evident by its higher HOMO energy, lower HOMO (D) - LUMO (A) gap (ΔE), and favourable global reactivity descriptors. The enhanced donor ability is attributed to methyl substitution, which increases electron density and facilitates stronger interactions with the electron-deficient acceptor. Experimental results, including higher formation constants and molar extinction coefficients, further confirmed that the resulting complexes were stable, particularly in dichloromethane. These findings highlighted the significant impact of structural modifications on donor strength and CT complex formation, offering valuable insights for the design of advanced donor-acceptor systems in optoelectronic and sensing applications.

Acknowledgement

The infrastructural financial support under CURIE programme from the WISE-KIRAN division of Department of Science and Technology, New Delhi, India to IIS (deemed to be University), Jaipur, India (File No. DST/CURIE-02/2023/IISU) is gratefully acknowledged.

Declaration

Author Contributions

Pratibha Mittal: Conceptualization, investigations data compilation, formal analysis, writing original Draft.

Dr. Manisha Patni: Supervision, Final Review.

Dr. Raakhi Gupta: Co-supervision.

The final manuscript was reviewed and endorsed by all authors.

Disclosure and Conflict of Interest

The authors confirm absence of financial, personal, or other relationships that might affect the findings or their interpretation.

Funding Information

No specific funding was provided for this research by public, commercial, or nonprofit organizations.

References

- [1] R. S. Mulliken, "Structures of Complexes Formed by Halogen Molecules with Aromatic and with Oxygenated Solvents1," J. Am. Chem. Soc., vol. 72, no. 1, pp. 600–608, Jan. 1950, doi: 10.1021/ja01157a151.
- [2] R. S. Mulliken, "The interaction of electron donors and acceptors," J. Chim. Phys., vol. 61, pp. 20–38, 1964, doi: 10.1051/jcp/1964610020.
- [3] E. M. Kosower, "Molecular Interaction: Organic Charge-Transfer Complexes . R. Foster. Academic Press, New York, 1969. xii, 472 pp., illus. \$22.50. Organic Chemistry, vol. 15.," Science, vol. 170, no. 3962, pp. 1076–1076, Dec. 1970, doi: 10.1126/science.170.3962.1076.a.
- [4] W. Wang, L. Luo, P. Sheng, J. Zhang, and Q. Zhang, "Multifunctional Features of Organic Charge-Transfer Complexes: Advances and Perspectives," Chem. Eur. J., vol. 27, no. 2, pp. 464–490, Jan. 2021, doi: 10.1002/chem.202002640.
- [5] D. Shen, W.-C. Chen, M.-F. Lo, and C.-S. Lee, "Charge-transfer complexes and their applications in optoelectronic devices," Mater. Today Energy, vol. 20, p. 100644, Jun. 2021, doi: 10.1016/j.mtener.2021.100644.
- [6] M. Baharfar, A. C. Hillier, and G. Mao, "Charge-Transfer Complexes: Fundamentals and Advances in Catalysis, Sensing, and Optoelectronic Applications," Adv. Mater., p. 2406083, Jul. 2024, doi: 10.1002/adma.202406083.
- [7] B. R. Hood et al., "Synthesis and Optical and Nonlinear Optical Properties of Linear and Two-Dimensional Charge Transfer Chromophores Based on Polyoxometalates," Inorg. Chem., vol. 63, no. 51, pp. 24250–24261, Dec. 2024, doi: 10.1021/acs.inorgchem.4c04179.
- [8] S. Naskar and M. Das, "The effect of metal-to-ligand charge transfer on linear and nonlinear optical properties of hexaphyrin and metallo-hexaphyrins," Mol. Phys., vol. 123, no. 9, p. e2386385, May 2025, doi:10.1080/00268976.2024.2386385.
- [9] K. Mohammedsaleh Katubi, M. Saqib, M. Sulaman, Z. A. Alrowaili, and M. S. Al-Buriahi, "Designing high-efficiency organic semi-conductors for organic photodetectors assisted by machine learning and property prediction," Chem. Phys., vol. 582, p. 112295, Jun. 2024, doi: 10.1016/j.chemphys.2024.112295.
- [10] T. Ng, Q. Yang, H. Mo, M. Lo, W. Zhang, and C. Lee, "Wide-Spectral Photoresponse of Black Molybdenum Oxide Photodetector via Sub-Bandgap Electronic Transition," Adv. Opt. Mater., vol. 1, no. 10, pp. 699–702, Oct. 2013, doi: 10.1002/adom.201300220.

- [11] M. Li, X. Zhou, W. Ding, S. Guo, and N. Wu, "Fluorescent aptamer-functionalized graphene oxide biosensor for label-free detection of mercury(II)," Biosens. Bioelectron., vol. 41, pp. 889–893, Mar. 2013, doi: 10.1016/j.bios.2012.09.060.
- [12] K. Song, S.-J. Hwang, Y. Jeon, and Y. Yoon, "The Biomedical Applications of Biomolecule Integrated Biosensors for Cell Monitoring," Int. J. Mol. Sci., vol. 25, no. 12, p. 6336, Jun. 2024, doi: 10.3390/ijms25126336.
- [13] H. J. Wörner et al., "Charge migration and charge transfer in molecular systems," Struct. Dyn., vol. 4, no. 6, Nov. 2017, doi: 10.1063/1.4996505.
- [14] W. Huang et al., "Trapping highly reactive photoinduced charge-transfer complex between amine and imide by light," Chem, vol. 10, no. 9, pp. 2829– 2843, Sep. 2024, doi: 10.1016/j.chempr.2024.05.005.
- [15] S. Wang, N. Hu, Y. Huang, and W. Deng, "Charge-transfer complex promotes energy storage performance of single-moiety organic electrode materials in aqueous zinc-ion battery at low temperatures," Appl. Surf. Sci., vol. 619, p. 156725, May 2023, doi: 10.1016/j.apsusc.2023.156725.
- [16] "Organic Electronic Memory Devices," in Electrical Memory Materials and Devices, The Royal Society of Chemistry, 2015, pp. 1–53. doi: 10.1039/9781782622505-00001.
- [17] C. Mathur, R. Gupta, and R. K. Bansal, "Organic Donor-Acceptor Complexes As Potential Semiconducting Materials," Chem. – Eur. J., vol. 30, no. 23, Apr. 2024, doi: 10.1002/chem.202304139.
- [18] M.-A. Codescu et al., "Ultrafast Proton Transfer Pathways Mediated by Amphoteric Imidazole," J. Phys. Chem. Lett., vol. 14, no. 20, pp. 4775–4785, May 2023, doi: 10.1021/acs.jpclett.3c00595.
- [19] F.-R. Lin, Z.-Y. Liu, G.-Q. Zhang, J. Zhang, and X.-M. Ren, "Understanding proton conduction enhancement of MOF-802 through in situ incorporation of imidazole into its channels," Inorg. Chem. Commun., vol. 157, p. 111340, Nov. 2023, doi: 10.1016/j.inoche.2023.111340.
- [20] D. Tzaras, M. Voigtländer, B. M. Zimmermann, T. Rüffer, and J. F. Teichert, "Synthesis of a Library of Bifunctional N-Heterocyclic Carbene Ligand Precursors with Hydrogen Bond Donor Subunits," Eur. J. Org. Chem., vol. 28, no. 27, p. e202500389, Jul. 2025, doi: 10.1002/ejoc.202500389.
- [21] R. Silva Moratório De Moraes et al., "An overview on generation and general properties of N-heterocyclic carbenes: Applications of 1,2,4-triazolium carbenes as metal free organocatalysts," Arab. J. Chem., vol. 17, no. 2, p. 105527, Feb. 2024, doi: 10.1016/j.arabjc.2023.105527.
- [22] K. T. Movellan, M. Wegstroth, K. Overkamp, A. Leonov, S. Becker, and L. B. Andreas, "Imidazole-Imidazole Hydrogen Bonding in the pH-Sensing Histidine Side Chains of Influenza A M2," J. Am. Chem. Soc., vol. 142, no. 6, pp. 2704–2708, Feb. 2020, doi: 10.1021/jacs.9b10984.
- [23] E. Yu. Tupikina, M. V. Sigalov, O. Alkhuder, and P. M. Tolstoy, "Charge Relay Without Proton Transfer: Coupling of Two Short Hydrogen Bonds via Imidazole in Models of Catalytic Triad of Serine Protease Active Site," ChemPhysChem, vol. 25, no. 12, p. e202300970, Jun. 2024, doi: 10.1002/ cphc.202300970.

- [24] Z. Li et al., "Simulating Metal-Imidazole Complexes," J. Chem. Theory Comput., vol. 20, no. 15, pp. 6706–6716, Aug. 2024, doi: 10.1021/acs.jctc.4c00581.
- [25] X.-W. Zhu, D. Luo, X.-P. Zhou, and D. Li, "Imidazole-based metal-organic cages: Synthesis, structures, and functions," Coord. Chem. Rev., vol. 455, p. 214354, Mar. 2022, doi: 10.1016/j.ccr.2021.214354.
- [26] L. Vrban et al., "Proton and Metal Dication Affinities of Tetracyclic Imidazo[4,5-b]Pyridine-Based Molecules: Insights from Mass Spectrometry and DFT Analysis," Molecules, vol. 30, no. 13, p. 2684, Jun. 2025, doi: 10.3390/ molecules30132684.
- [27] J. Żygowska, M. Orlikowska, I. Zhukov, W. Bal, and A. Szymańska, "Copper interaction with cystatin C: effects on protein structure and oligomerization," FEBS J., vol. 291, no. 9, pp. 1974–1991, May 2024, doi: 10.1111/febs.17092.
- [28] P. Sharma, C. LaRosa, J. Antwi, R. Govindarajan, and K. A. Werbovetz, "Imidazoles as Potential Anticancer Agents: An Update on Recent Studies," Molecules, vol. 26, no. 14, p. 4213, Jul. 2021, doi: 10.3390/molecules26144213.
- [29] H. A. Al-Ghamdi et al., "Synthesis and Biological Evaluation of Novel Imidazole Derivatives as Antimicrobial Agents," Biomolecules, vol. 14, no. 9, p. 1198, Sep. 2024, doi: 10.3390/biom14091198.
- [30] K. Elgammal and M. Maußner, "A Quantum Computing Approach to Simulating Corrosion Inhibition," 2024, arXiv. doi: 10.48550/ARXIV.2412.00951.
- [31] N. Sharma, M. Kour, R. Gupta, and R. K. Bansal, "A new cross-conjugated mesomeric betaine," RSC Adv., vol. 11, no. 41, pp. 25296-25304, 2021, doi: 10.1039/D1RA03981D.
- H. Wang, T. Lu, T. He, and D. Chen, "Theoretical Studies on the Structure and Spectrum of Imidazole-Chloranil Charge Transfer Complex," Chin. J. Chem. Phys., vol. 21, no. 6, pp. 560-568, Dec. 2008, doi: 10.1088/1674-0068/21/06/560-568.
- [33] T. Murata, Y. Morita, Y. Yakiyama, and K. Nakasuji, "Synthesis, crystal structure, and charge-transfer complexes of TTF derivatives having two imidazole hydrogen-bonding units," Phys. B Condens. Matter, vol. 405, no. 11, pp. S41-S44, Jun. 2010, doi: 10.1016/j.physb.2009.10.022.
- [34] K. Alam and I. M. Khan, "Crystallographic, dynamic and Hirshfeld surface studies of charge transfer complex of imidazole as a donor with 3,5-dinitrobenzoic acid as an acceptor: Determination of various physical parameters," Org. Electron., vol. 63, pp. 7-22, Dec. 2018, doi: 10.1016/j. orgel.2018.08.037.
- [35] Y. Morita, T. Murata, and K. Nakasuji, "Cooperation of Hydrogen-Bond and Charge-Transfer Interactions in Molecular Complexes in the Solid State," Bull. Chem. Soc. Jpn., vol. 86, no. 2, pp. 183-197, Feb. 2013, doi: 10.1246/ bcsj.20120241.
- I. M. Khan, K. Alam, M. J. Alam, and M. Ahmad, "Spectrophotometric and photocatalytic studies of H-bonded charge transfer complex of oxalic acid with imidazole: single crystal XRD, experimental and DFT/TD-DFT studies," New J. Chem., vol. 43, no. 23, pp. 9039–9051, 2019, doi: 10.1039/C9NJ00332K.

- [37] L. Miyan, S. Qamar, and A. Ahmad, "Synthesis, characterization and spectrophotometric studies of charge transfer interaction between donor imidazole and π acceptor 2,4-dinitro-1-naphthol in various polar solvents," J. Mol. Liq., vol. 225, pp. 713–722, Jan. 2017, doi: 10.1016/j.molliq.2016.10.126.
- [38] A. Mostafa and H. S. Bazzi, "Synthesis and spectroscopic studies on charge-transfer molecular complexes formed in the reaction of imidazole and 1-benzylimidazole with σ- and π-acceptors," Spectrochim. Acta. A. Mol. Biomol. Spectrosc., vol. 79, no. 5, pp. 1613–1620, Sep. 2011, doi: 10.1016/j. saa.2011.05.021.
- [39] T. Murata et al., "Hydrogen-Bond Interaction in Organic Conductors: Redox Activation, Molecular Recognition, Structural Regulation, and Proton Transfer in Donor—Acceptor Charge-Transfer Complexes of TTF-Imidazole," J. Am. Chem. Soc., vol. 129, no. 35, pp. 10837–10846, Sep. 2007, doi: 10.1021/ja072607m.
- [40] M. R. Ganjali, P. Norouzi, S. Shirvani-Arani, and A. Kakanezhadifard, "Synthesis of a charge-transfer complex of (1,3-diphenyldihydro-1H-imidazole)-4,5-dione dioxide with iodide and its application to the development of a highly selective and sensitive triiodide PVC-membrane electrode," J. Anal. Chem., vol. 62, no. 3, pp. 279–284, Mar. 2007, doi: 10.1134/S106193480703015X.
- [41] F. K. Bine, N. S. Tasheh, and J. N. Ghogomu, "A Quantum Chemical Screening of Two Imidazole-Chalcone Hybrid Ligands and Their Pd, Pt and Zn Complexes for Charge Transport and Nonlinear Optical (NLO) Properties: A DFT Study," Comput. Chem., vol. 09, no. 04, pp. 215–237, 2021, doi: 10.4236/ cc.2021.94012.
- [42] H. Demirhan, M. Arslan, M. Zengin, and M. Kucukislamoglu, "Investigation of Charge Transfer Complexes Formed between Mirtazapine and Somen-Acceptors," J. Spectrosc., vol. 2013, pp. 1–7, 2013, doi: 10.1155/2013/875953.
- [43] H. A. Benesi and J. H. Hildebrand, "A Spectrophotometric Investigation of the Interaction of Iodine with Aromatic Hydrocarbons," J. Am. Chem. Soc., vol. 71, no. 8, pp. 2703–2707, Aug. 1949, doi: 10.1021/ja01176a030.
- [44] K. M. Al-Ahmary, M. M. El-Kholy, I. A. Al-Solmy, and M. M. Habeeb, "Spectroscopic studies and molecular orbital calculations on the charge transfer reaction between DDQ and 2-aminopyridine," Spectrochim. Acta. A. Mol. Biomol. Spectrosc., vol. 110, pp. 343–350, Jun. 2013, doi: 10.1016/j. saa.2013.03.055.
- [45] D. Vernez et al., "Airborne nano-TiO 2 particles: An innate or environmentally-induced toxicity?," J. Photochem. Photobiol. Chem., vol. 343, pp. 119–125, Jun. 2017, doi: 10.1016/j.jphotochem.2017.04.022.
- [46] J. M. Juma and S. A. Vuai, "Computational studies of the thermodynamic properties, and global and reactivity descriptors of fluorescein dye derivatives in acetonitrile using density functional theory," J. Chem. Res., vol. 45, no. 7–8, pp. 800–805, Jul. 2021, doi: 10.1177/1747519821994518.
- [47] B. Solanki, P. Sharma, P. Ranjan, P. Kumar, and T. Chakraborty, "A computational study of double perovskites A2BI6 (A=Cs, K, Rb; B=Pt, Sn) invoking density functional theory," J. Phys. Org. Chem., vol. 36, no. 12, Dec. 2023, doi: 10.1002/poc.4519.

Mittal et al. Spectrophotometric Investigations of Charge Transfer Complexes

- [48] J. Yu, N. Q. Su, and W. Yang, "Describing Chemical Reactivity with Frontier Molecular Orbitalets," JACS Au, vol. 2, no. 6, pp. 1383–1394, Jun. 2022, doi: 10.1021/jacsau.2c00085.
- [49] N. F. Al Harby, M. El Batouti, and E.-S. H. EL-mossalamy, "Molecular spectroscopic kinetic and computational studies on charge transfer complexes of dibenzothiophene azomethine with nitrobenzene as π-acceptors and its antibacterial effect," Polym. Bull., vol. 81, no. 5, pp. 3995–4012, Apr. 2024, doi: 10.1007/s00289-024-05145-9.